

Quantum Algorithm for Dynamic Mode Decomposition and Matrix Eigenvalue Decomposition with Complex Eigenvalues

Yuta Mizuno^{1, 2, 3, *} and Tamiki Komatsuzaki^{1, 2, 3, 4}

¹Research Institute for Electronic Science, Hokkaido University Sapporo, Hokkaido 001-0020, Japan

²Institute for Chemical Reaction Design and Discovery (WPI-ICReDD),

Hokkaido University, Sapporo, Hokkaido 001-0021, Japan

³Graduate School of Chemical Sciences and Engineering,

Hokkaido University, Sapporo, Hokkaido 060-8628, Japan

⁴The Institute of Scientific and Industrial Research,

Osaka University, Ibaraki, Osaka 567-0047, Japan

(Dated: October 30, 2023)

We present a quantum algorithm that analyzes time series data simulated by a quantum differential equation solver. The proposed algorithm is a quantum version of the dynamic mode decomposition algorithm used in diverse fields such as fluid dynamics and epidemiology. Our quantum algorithm can also extract matrix eigenvalues by analyzing the corresponding linear dynamical system. Our algorithm handles a broader range of matrices with complex eigenvalues, unlike existing efficient quantum eigensolvers limited to specific matrix types. The complexity of our quantum algorithm is $O(\text{poly log } N)$ for an N -dimensional system. This is an exponential speedup over known classical algorithms with at least $O(N)$ complexity. Thus, our quantum algorithm is expected to enable high-dimensional dynamical system analysis and large matrix eigenvalue decomposition, intractable for classical computers.

I. INTRODUCTION

Quantum algorithms provide exponential speedup over classical algorithms for numerical linear algebra tasks such as eigenvalue decomposition of unitary or Hermitian matrices [1–3], singular value decomposition of low-rank matrices [4, 5], and solving linear systems of equations [6, 7]. These quantum algorithms can solve problems of N dimensions in runtime $O(\text{poly log } N)$. They have significant applications in quantum chemistry [8], machine learning [4, 9], and solving differential equations [10–13].

Quantum numerical linear algebra also offers prospects for advancements in dynamical system analysis. A probability density function on the state space of a dynamical system is advanced in time by the Perron–Frobenius operator [14, 15]. Meanwhile, the Koopman operator is responsible for the time evolution of observable functions on the state space [14, 15]. These operators are linear operators on infinite dimensional function spaces. In other words, any finite-dimensional (possibly nonlinear) dynamical system can be described as an infinite-dimensional linear dynamical system. To analyze such an infinite-dimensional system, one may resort to a finite-dimensional approximation. This often leads to a linear system with an extremely-large number of dimensions $N (\gg 1)$. Such systems may be simulated using a quantum linear differential equation solver (QLDES) [10–12] in runtime $O(\text{poly log } N)$. The quantum solver yields a quantum state whose amplitudes encode time series data of the dynamical system. However, as the tomography of such quantum state takes a runtime of $O(N)$, an efficient

method for extracting essential, dynamical information from the quantum data is highly demanded.

We propose a novel quantum algorithm for dynamic mode decomposition (DMD), a numerical technique that estimates the spectral decomposition of the Koopman operator of a dynamical system from its time-series data [14]. This spectral decomposition elucidates the temporal behavior of the dynamical system. Classical DMD algorithms are frequently applied in various fields such as fluid dynamics and epidemiology [14]. Quantum algorithms for the spectral estimation from time-series data have been proposed by Steffens et al. [16] and Xue et al. [17]; however, these algorithms presuppose time-series data stored in a quantum random access memory or specific amplitude encoding, and efficiently preparing this data with a QLDES remains a challenge. Furthermore, such disconnection between simulation and time-series analysis on a quantum computer can be potentially an obstacle to exponential speedup achieved by each part. In contrast, our quantum DMD (qDMD) algorithm proposed in this article offers an implementable and seamless protocol to analyze QLDES-generated time-series data on a quantum computer. Consequently, our algorithm fills the critical gap in simulation and data analysis, achieving an exponential speedup over classical algorithms with respect to the system’s dimension N .

Our qDMD algorithm can also serve as a quantum subroutine for eigenvalue decomposition of matrices, especially those with complex eigenvalues. If a linear differential equation $\dot{\mathbf{x}} = \mathbf{A}\mathbf{x}$ can be simulated efficiently on a quantum computer, our algorithm can efficiently compute approximate eigenvalues and eigenvectors of $\exp(\Delta t \mathbf{A})$, where Δt is the time step of the simulation. Notably, the matrix \mathbf{A} is not restricted to Hermitian and may have complex eigenvalues. Therefore, the composite

* mizuno@es.hokudai.ac.jp

protocol of a QLDES and our qDMD algorithm can be considered as a generalization of quantum phase estimation [1–3], which combines Hamiltonian simulation and quantum Fourier transform. Although previous studies [18–21] have attempted to develop quantum eigensolvers for complex eigenvalue problems, these approaches have limitations such as the lack of the theoretical guarantee of an exponential speedup [18–20] and requiring a specific form of input states [21]. Our qDMD algorithm is designed to be free from such limitations.

II. DYNAMIC MODE DECOMPOSITION

We introduce the *exact DMD* algorithm proposed by Tu et al. [22]. Let us consider an N -dimensional linear dynamical system $\dot{\mathbf{x}} = \mathbf{A}\mathbf{x}$, where $\mathbf{x} \in \mathbb{C}^N$, and $\mathbf{A} \in \mathbb{C}^{N \times N}$ is a diagonalizable matrix¹. Let \mathbf{K} denote the time evolution operator with time step Δt : $\mathbf{K} := \exp(\Delta t \mathbf{A})$. Suppose we have a collection of M snapshot pairs of time-series data, symbolized as $\{(\mathbf{x}_j, \mathbf{x}'_j)\}_{j=0}^{M-1}$. Here \mathbf{x}'_j signifies the state observed at the subsequent time step following \mathbf{x}_j : $\mathbf{x}'_j \approx \mathbf{K}\mathbf{x}_j$ ². Note that \mathbf{x}_j 's can be taken from multiple different trajectories. From the data, we can estimate the time-evolution operator \mathbf{K} as

$$\tilde{\mathbf{K}} = \underset{\mathbf{J} \in \mathbb{C}^{N \times N}}{\operatorname{argmin}} \|\mathbf{X}' - \mathbf{J}\mathbf{X}\|_{\text{F}} = \mathbf{X}'\mathbf{X}^+, \quad (1)$$

where $\tilde{\mathbf{K}}$ signifies the approximation of the underlying \mathbf{K} , $\|\cdot\|_{\text{F}}$ denotes the Frobenius norm, $\mathbf{X} := [\mathbf{x}_0 \cdots \mathbf{x}_{M-1}]$, $\mathbf{X}' := [\mathbf{x}'_0 \cdots \mathbf{x}'_{M-1}]$, and \mathbf{X}^+ is the pseudo-inverse of \mathbf{X} . The construction of $N \times N$ matrix $\tilde{\mathbf{K}}$ and its eigenvalue decomposition becomes intractable as N increases. Thus, we solve the eigenvalue problem of the following projected matrix instead:

$$\tilde{\mathbf{K}}' = \mathbf{Q}^\dagger \tilde{\mathbf{K}} \mathbf{Q}, \quad (2)$$

where \mathbf{Q} is an $N \times R$ matrix whose columns are the R dominant left singular vectors of the $N \times 2M$ matrix $[\mathbf{X} \ \mathbf{X}']$. The effective rank R is determined so that the error of the rank- R approximation of $[\mathbf{X} \ \mathbf{X}']$ in the Frobenius norm is less than a specified tolerance. The exact DMD algorithm assumes that R is sufficiently smaller than N so that the eigenvalue decomposition of the $R \times R$ matrix $\tilde{\mathbf{K}}'$ can be computed practically on a classical computer. The eigenvalue decomposition of $\tilde{\mathbf{K}}'$ approximates that of $\tilde{\mathbf{K}}$ as

$$\tilde{\lambda}_r \approx \lambda'_r, \quad \tilde{\mathbf{w}}_r \approx \mathbf{Q}\tilde{\mathbf{w}}'_r \quad (r = 1, \dots, R). \quad (3)$$

Here, $\tilde{\lambda}_r$ and $\tilde{\mathbf{w}}_r$ (resp. λ'_r and $\tilde{\mathbf{w}}'_r$) are the r -th eigenvalue and eigenvector of $\tilde{\mathbf{K}}$ (resp. $\tilde{\mathbf{K}}'$). The real part and the imaginary part of $(\ln \tilde{\lambda}_r)/\Delta t$ correspond to the decay/growth rate and the oscillation frequency of the r -th DMD mode, respectively. The computational complexity of this algorithm is $O(\min(NM^2, MN^2))$ for the singular value decomposition (SVD) and $O(R^3)$ for the eigenvalue decomposition of $\tilde{\mathbf{K}}'$ [23].

III. QDMD ALGORITHM

Our qDMD algorithm consists of the following five steps:

1. Prepare quantum states encoding \mathbf{X} and \mathbf{X}' using a QLDES.
2. Compute the SVDs of \mathbf{X} , \mathbf{X}' , and $[\mathbf{X} \ \mathbf{X}']$ on a quantum computer.
3. Estimate the elements of $\tilde{\mathbf{K}}'$ from the quantum data and construct $\tilde{\mathbf{K}}'$ as classical data.
4. Solve the eigenvalue problem of $\tilde{\mathbf{K}}'$ on a classical computer.
5. Compute a quantum state encoding $\tilde{\mathbf{w}}_r$.

Steps 1–3, and 5 are efficiently executed on a quantum computer in runtime $O(\text{poly log } N)$ as shown below. Given that $R \ll N$, step 4 can be handled by a classical computer. Consequently, our qDMD algorithm is exponentially faster than its classical counterpart with respect to N . Similar quantum-classical hybrid strategies are also employed by Steffens et al. [16] and Xue et al. [17], though the specifics of the quantum procedures differ.

In what follows, we will expound the quantum procedures of steps 1–3 and 5. Henceforth, we adopt the following notation: The computational basis whose bit string represents integer i is denoted by $|i\rangle$. As necessary, we denote a ket vector of the k -th quantum register like $| \rangle_k$. For vector $\mathbf{v} = (v^0, \dots, v^{n-1})^\top \in \mathbb{C}^n$, we define $|\mathbf{v}\rangle := \sum_{i=0}^{n-1} v^i |i\rangle$. Similarly, for matrix $\mathbf{Z} = [\mathbf{v}_0 \cdots \mathbf{v}_{m-1}] \in \mathbb{C}^{n \times m}$, we write $|\mathbf{Z}\rangle := \sum_{j=0}^{m-1} |\mathbf{v}_j\rangle |j\rangle = \sum_{i=0}^{n-1} \sum_{j=0}^{m-1} v_j^i |i\rangle |j\rangle$. A normalized matrix $\mathbf{Z}/\|\mathbf{Z}\|_{\text{F}}$ is denoted by $\hat{\mathbf{Z}}$, thus $|\hat{\mathbf{Z}}\rangle$ symbolizes the normalized ket vector (quantum state) proportional to $|\mathbf{Z}\rangle$. Additionally, the r -th singular value, left and right singular vectors of matrix \mathbf{Z} are designated by $\sigma_r^{\mathbf{Z}}$, $\mathbf{u}_r^{\mathbf{Z}}$, and $\mathbf{v}_r^{\mathbf{Z}}$, respectively. The notation of quantum circuit diagrams we employ can be found in [24].

A. Step 1

The quantum circuit shown in Fig. 1 is responsible for preparing the quantum state encoding \mathbf{X} and \mathbf{X}' . Here, we prepare time-series data of L different trajectories of $(T+1)$ time steps. Consequently, the number of columns M equals $(T+1)L$ in this article.

¹ For the case that A is not diagonalizable, see discussion in Supplemental Material.

² Since numerical integration of a linear differential equation involves approximations, the simulated data \mathbf{x}'_j is an approximation of the exact solution $\mathbf{K}\mathbf{x}_j$.

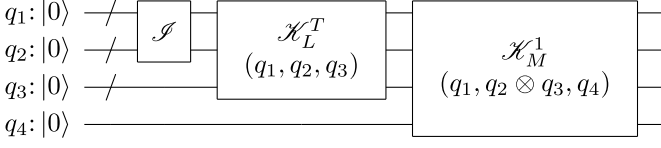


FIG. 1. Quantum circuit for data matrix preparation. \mathcal{J} is a quantum oracle for initial state preparation. \mathcal{K}_μ^τ is a quantum algorithm that simulates the dynamics up to the τ -th time step for μ initial conditions. The label of each of the simulation gate indicates which registers the gate acts on; e.g, label (q_i, q_k, q_t) indicates that the simulation gate is performed on the registers q_i , q_k , and q_t , which correspond to the first, second, and third registers in Eq. 5, respectively.

We assume a quantum oracle \mathcal{J} that generates a superposition of L initial states $\{\mathbf{x}_k\}_{k=0}^{L-1}$ as

$$|0\rangle|0\rangle \xrightarrow{\mathcal{J}} \sum_{k=0}^{L-1} |\mathbf{x}_k\rangle|k\rangle. \quad (4)$$

Here, the normalizing constant for the right hand side is omitted. We also introduce a quantum subroutine \mathcal{K}_μ^τ that simulates the linear dynamical system up to a specified time step τ for μ initial conditions:

$$\sum_{k=0}^{\mu-1} |\mathbf{x}_k\rangle|k\rangle|0\rangle \xrightarrow{\mathcal{K}_\mu^\tau} \sum_{k=0}^{\mu-1} \sum_{t=0}^{\tau} |\tilde{\mathbf{x}}_k(t \Delta t)\rangle|k\rangle|t\rangle, \quad (5)$$

where $\tilde{\mathbf{x}}_k(t \Delta t)$ is the simulated state at the t -th time step of the trajectory initiated from \mathbf{x}_k , and the normalizing constants for the both sides are omitted. We can implement \mathcal{K}_μ^τ by the Taylor series method and a quantum linear systems solver with gate complexity $O(\tau \text{poly log}(N\tau\mu/\epsilon))$ [11, 25], where ϵ denotes the tolerance for simulation error.

Applying \mathcal{J} and \mathcal{K}_L^τ to registers q_1 , q_2 , and q_3 , we get

$$|\mathbf{X}\rangle = \sum_{k=0}^{L-1} \sum_{t=0}^T |\tilde{\mathbf{x}}_k(t \Delta t)\rangle_1 |t + (T+1)k\rangle_{23}. \quad (6)$$

In this context, the register q_1 encodes states of the dynamical system, and the registers q_2 and q_3 —indicating the initial condition k and the time step t —collectively label the column index of \mathbf{X} as $|t + (T+1)k\rangle_{23} = |k\rangle_2 |t\rangle_3$. Regarding the M columns of \mathbf{X} as initial states and the register q_4 as the time step counter, the one-step simulation gate \mathcal{K}_M^1 generates the quantum state proportional to

$$|\mathbf{X} \mathbf{X}'\rangle = |\mathbf{X}\rangle|0\rangle_4 + |\mathbf{X}'\rangle|1\rangle_4. \quad (7)$$

This ket vector can be viewed as encoding $[\mathbf{X} \mathbf{X}']$, regarding $q_2 \otimes q_3 \otimes q_4$ as indicating the column index collectively. Measuring the fourth register, we obtain a quantum state $|\hat{\mathbf{X}}\rangle$ or $|\hat{\mathbf{X}}'\rangle$.

B. Step 2

According to the procedure proposed by Schuld et al. [9], we perform the SVD of a normalized matrix $\hat{\mathbf{Z}}$ ($\mathbf{Z} = \mathbf{X}$, \mathbf{X}' , or $[\mathbf{X} \mathbf{X}']$) on a quantum computer using C copies of $|\hat{\mathbf{Z}}\rangle$ as

$$|\hat{\mathbf{Z}}\rangle^{\otimes C} \mapsto |\text{SVD}(\hat{\mathbf{Z}})\rangle \approx \sum_{r=1}^R \hat{\sigma}_r^{\mathbf{Z}} |\mathbf{u}_r^{\mathbf{Z}}\rangle |\mathbf{v}_r^{\mathbf{Z}^*}\rangle |(\hat{\sigma}_r^{\mathbf{Z}})^2\rangle_5, \quad (8)$$

where $\hat{\sigma}_r^{\mathbf{Z}} := \sigma_r^{\mathbf{Z}} / \|\mathbf{Z}\|_{\text{F}}$, and $|(\hat{\sigma}_r^{\mathbf{Z}})^2\rangle_5$ designates the computational basis of the extra fifth register indicating the binary representation of $(\hat{\sigma}_r^{\mathbf{Z}})^2$. This process utilizes density matrix exponentiation [4] and quantum phase estimation. The necessary number of state copies C for precision ϵ is $O(1/\epsilon^2)$ [26].

C. Step 3

The estimation of $\hat{\mathbf{K}}'$ is based on the following factorization:

$$\hat{\mathbf{K}}' \approx \frac{\|\mathbf{X}'\|_{\text{F}}}{\|\mathbf{X}\|_{\text{F}}} (\mathbf{Q}^\dagger \mathbf{U}') \hat{\Sigma}' (\mathbf{V}'^\dagger \mathbf{V}) \hat{\Sigma}^{-1} (\mathbf{U}'^\dagger \mathbf{Q}), \quad (9)$$

where $\hat{\mathbf{X}} \approx \mathbf{U} \hat{\Sigma} \mathbf{V}^\dagger$ and $\hat{\mathbf{X}}' \approx \mathbf{U}' \hat{\Sigma}' \mathbf{V}'^\dagger$ are the SVDs of the normalized data matrices with rank- R truncation. The first factor $\|\mathbf{X}'\|_{\text{F}} / \|\mathbf{X}\|_{\text{F}}$ ($= \|\mathbf{X}'\| / \|\mathbf{X}\|$) can be estimated by measuring the fourth register of $|\mathbf{X} \mathbf{X}'\rangle$ because the probability ratio of measured values 1 to 0, $\text{Pr}(q_4 = 1) / \text{Pr}(q_4 = 0)$, equals the square of this factor. The diagonal elements of $\hat{\Sigma}$ and $\hat{\Sigma}'$, i.e., $\{\hat{\sigma}_r^{\mathbf{X}}\}_{r=1}^R$ and $\{\hat{\sigma}_r^{\mathbf{X}'}\}_{r=1}^R$, can be estimated by measuring the fifth register of $|\text{SVD}(\hat{\mathbf{X}})\rangle$ and $|\text{SVD}(\hat{\mathbf{X}}')\rangle$. All the off-diagonal elements of $\hat{\Sigma}$ and $\hat{\Sigma}'$ are zero. The elements of matrices $\mathbf{Q}^\dagger \mathbf{U}'$, $\mathbf{U}'^\dagger \mathbf{Q}$, and $\mathbf{V}'^\dagger \mathbf{V}$ are inner products between singular vectors. Note that the r -th column vector of \mathbf{Q} corresponds to $\mathbf{u}_r^{[\mathbf{X} \mathbf{X}']}$. Now, the remaining task is to estimate $\langle \mathbf{u}_r^{[\mathbf{X} \mathbf{X}']} | \mathbf{u}_{r'}^{[\mathbf{X}']} \rangle$, $\langle \mathbf{u}_r^{\mathbf{X}} | \mathbf{u}_{r'}^{\mathbf{X}'} \rangle$, and $\langle \mathbf{v}_r^{\mathbf{X}'} | \mathbf{v}_{r'}^{\mathbf{X}} \rangle$ for R^2 combinations of r and r' .

The two-state SWAP test depicted in Fig. 2 (a) is often employed for estimating the absolute value of the inner product between arbitrary quantum states $|\psi_0\rangle$ and $|\psi_1\rangle$. However, the two-state SWAP test cannot estimate the phase (argument) of the inner product. Furthermore, the global phase of a singular vector is arbitrary. For instance, if we have a singular vector pair $(|\mathbf{u}_r\rangle, |\mathbf{v}_r^*\rangle)$, then $(e^{i\theta}|\mathbf{u}_r\rangle, e^{-i\theta}|\mathbf{v}_r^*\rangle)$ is also a valid pair, where θ ranges from 0 to 2π . The choice of the global phase of the singular vector pair changes inner products to be estimated. To overcome these challenges, we introduce the *three-state SWAP test* (Fig. 2 (b)) and *reference states* for the left and right singular vectors³.

³ We assume that the reference states can be computed by uni-

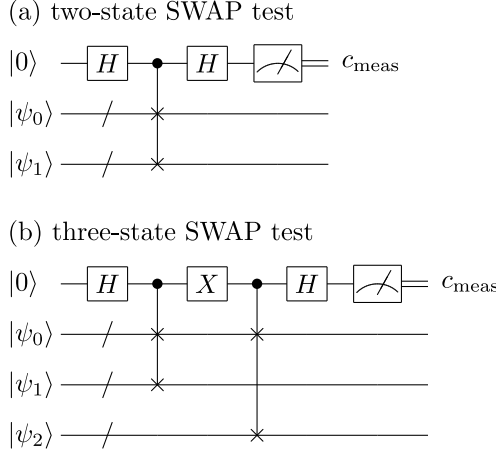


FIG. 2. Quantum circuit for inner product estimation using controlled SWAP gates. The input states $|\psi_k\rangle$ ($k = 0, 1, 2$) are arbitrary quantum states. (a) In the two-state SWAP test, $\Pr[c_{\text{meas}} = 0] - \Pr[c_{\text{meas}} = 1] = |\langle\psi_0|\psi_1\rangle|^2$. (b) In the three-state SWAP test, $\Pr[c_{\text{meas}} = 0] - \Pr[c_{\text{meas}} = 1] = \text{Re}(\langle\psi_0|\psi_1\rangle\langle\psi_1|\psi_2\rangle\langle\psi_2|\psi_0\rangle)$. When the phase gate S^\dagger is inserted after the first Hadamard gate, $\Pr[c_{\text{meas}} = 0] - \Pr[c_{\text{meas}} = 1] = \text{Im}(\langle\psi_0|\psi_1\rangle\langle\psi_1|\psi_2\rangle\langle\psi_2|\psi_0\rangle)$.

First, we estimate the inner products between left sin-

gular vectors. We define the global phase of each left singular vector state $|\mathbf{u}\rangle$ such that $\arg\langle\chi_1|\mathbf{u}\rangle = 0$ for a fixed reference quantum state $|\chi_1\rangle$. The two-state SWAP test between $|\chi_1\rangle$ and $|\mathbf{u}\rangle$ estimates $|\langle\chi_1|\mathbf{u}\rangle|$. Here, the singular vector state $|\mathbf{u}\rangle$ can be prepared by executing the quantum SVD and measuring the fifth register encoding squared singular values. Additionally, the three-state SWAP test between $|\chi_1\rangle$ and arbitrary left singular vector states $|\mathbf{u}\rangle$ and $|\mathbf{u}'\rangle$ provides an estimate of $\langle\chi_1|\mathbf{u}\rangle\langle\mathbf{u}|\mathbf{u}'\rangle\langle\mathbf{u}'|\chi_1\rangle$. Leveraging the known absolute values and phases of $\langle\chi_1|\mathbf{u}\rangle$ and $\langle\mathbf{u}'|\chi_1\rangle$, we can derive an estimate of $\langle\mathbf{u}|\mathbf{u}'\rangle$. In this way, $\langle\mathbf{u}_r^{[\mathbf{X} \mathbf{X}']}|\mathbf{u}_{r'}^{[\mathbf{X} \mathbf{X}']}\rangle$ and $\langle\mathbf{u}_r^{[\mathbf{X} \mathbf{X}']}|\mathbf{u}_{r'}^{[\mathbf{X} \mathbf{X}']}\rangle$ can be estimated.

Next, we estimate the inner products between right singular vectors. Since the global phase of a right singular vector is synchronized with that of the associated left singular vector, we cannot arbitrary define $\arg\langle\chi_2|\mathbf{v}^*\rangle$ for a fixed reference state $|\chi_2\rangle$ and a right singular vector state $|\mathbf{v}^*\rangle$; instead, we also need to estimate $\arg\langle\chi_2|\mathbf{v}^*\rangle$. Once we determine $\langle\chi_2|\mathbf{v}^*\rangle$ for every right singular vector \mathbf{v} , we can estimate $\langle\mathbf{v}_r^{[\mathbf{X} \mathbf{X}']}|\mathbf{v}_{r'}^{[\mathbf{X} \mathbf{X}']}\rangle$ using the two-state and three-state SWAP tests as described above. Thus, let us consider how to determine $\langle\chi_2|\mathbf{v}^*\rangle$. First, we prepare the following quantum state using the quantum circuit depicted in Fig. 3 with applying the Step2 gate conditionally on $q_4 = 0$:

$$\frac{1}{\sqrt{2}\|[\mathbf{X} \mathbf{X}']\|_{\text{F}}} \left[\sum_{r=1}^R \sigma_r^{\mathbf{X}} |\mathbf{u}_r^{\mathbf{X}}\rangle_1 |\mathbf{v}_r^{\mathbf{X}^*}\rangle_{23} |0\rangle_4 |(\hat{\sigma}_r^{\mathbf{X}})^2\rangle_5 + |\mathbf{X}'\rangle_{123} |1\rangle_4 |0\rangle_5 \right] |0\rangle_6 + \frac{1}{\sqrt{2}} |\chi_1\rangle_1 |\chi_2\rangle_{23} |0\rangle_4 |0\rangle_5 |1\rangle_6. \quad (10)$$

Next, we input this state to the circuit shown in Fig. 4. The upper quantum register of the circuit corresponds to $q_1 \otimes q_2 \otimes q_3$ and the bottom corresponds to $q_4 \otimes q_5 \otimes q_6$. Let us set $|0\rangle_4|0\rangle_5|1\rangle_6$ and $|0\rangle_4|(\hat{\sigma}_r^{\mathbf{X}})^2\rangle_5|0\rangle_6$ to $|i\rangle$ and $|j\rangle$ in the circuit diagram, respectively. Then, the circuit provides an estimate of $\langle\chi_1|\mathbf{u}_r^{\mathbf{X}}\rangle\langle\chi_2|\mathbf{v}_r^{\mathbf{X}^*}\rangle$. Since we know the value of $\langle\chi_1|\mathbf{u}_r^{\mathbf{X}}\rangle$, we can derive an estimate of $\langle\chi_2|\mathbf{v}_r^{\mathbf{X}^*}\rangle$. Likewise, we can estimate $\langle\chi_2|\mathbf{v}_r^{\mathbf{X}^*}\rangle$ with applying the Step2 gate conditionally on $q_4 = 1$ in the circuit of Fig. 3.

The number of quantum SVDs necessary for estimating $\tilde{\mathbf{K}'}$ with precision ϵ is $O(1/\epsilon^2 \text{poly } R)$, excluding reference state preparation costs (see Supplemental Material). The factor $O(1/\epsilon^2)$ originates from sampling errors obeying the central limit theorem. While preparing the reference states may require additional $O(M)$ quantum SVDs, the overall gate complexity remains at $O(\text{poly log } N)$ (see Supplemental Material).

tary quantum circuits. We provide an example of a method for preparing reference states in Supplemental Material.

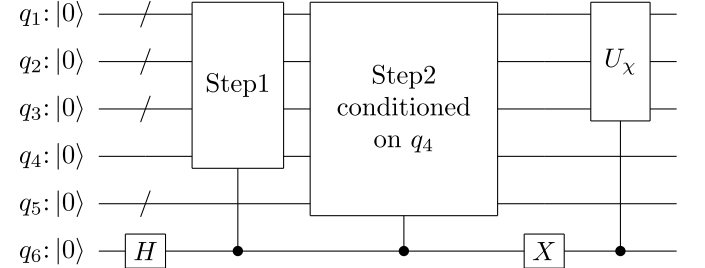


FIG. 3. Quantum circuit for generating input states for the circuit of Fig. 4. The Step1 gate generates $[[\mathbf{X} \mathbf{X}']]$. When the Step2 gate is applied conditioned on $q_4 = 0$ (resp. $q_4 = 1$), this gate performs the quantum SVD of $\hat{\mathbf{X}}$ (resp. $\hat{\mathbf{X}}'$). The unitary gate U_x creates the reference states as $U_x |0\rangle_1 |0\rangle_{23} = |\chi_1\rangle_1 |\chi_2\rangle_{23}$.

D. Step 5

From the eigenvalue decomposition of $\tilde{\mathbf{K}'}$ at step 4, we derive $\tilde{\mathbf{w}}_r'$. A quantum state encoding the r -th DMD

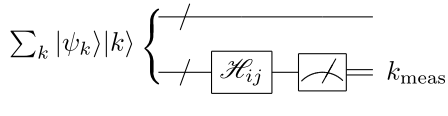


FIG. 4. Quantum circuit for inner product estimation using a Hadamard gate. Gate \mathcal{H}_{ij} is defined by $H_{ij} + I_{ij}^\perp$. Here, H_{ij} is the Hadamard gate on the 2-dimensional Hilbert space $\mathcal{H} := \text{span}\{|i\rangle, |j\rangle\}$, i.e., $H_{ij} := (|i\rangle\langle i| + |j\rangle\langle j| + |j\rangle\langle i| - |i\rangle\langle j|)/\sqrt{2}$, and I_{ij}^\perp is the identity operator on the orthogonal complementary space of \mathcal{H} . The $|\psi_k\rangle$'s are arbitrary unnormalized ket vectors. The measurement probability satisfies $\Pr[k_{\text{meas}} = i] - \Pr[k_{\text{meas}} = j] = 2 \text{Re} \langle \psi_i | \psi_j \rangle$. When the phase shift $|j\rangle \mapsto -i|j\rangle$ is applied before \mathcal{H}_{ij} , $\Pr[k_{\text{meas}} = i] - \Pr[k_{\text{meas}} = j] = 2 \text{Im} \langle \psi_i | \psi_j \rangle$.

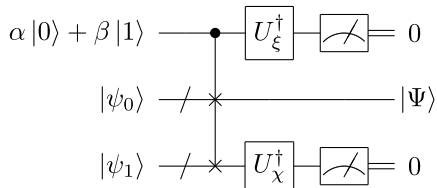


FIG. 5. Quantum circuit for coherent addition of two quantum states $|\psi_0\rangle$ and $|\psi_1\rangle$ [27]. U_χ is a unitary gate satisfying $U_\chi|0\rangle = |\chi\rangle$. U_ξ is a unitary gate satisfying $U_\xi|0\rangle = |\xi\rangle$, where $|\xi\rangle := \sqrt{c_0/(c_0 + c_1)}|0\rangle + \sqrt{c_1/(c_0 + c_1)}|1\rangle$. If the measured values of the first and third registers are both zero, the coherent addition has been successful.

mode is given by

$$|\tilde{w}_r\rangle = \sum_{r'=1}^R \tilde{w}_r^{r'} |w_{r'}^{[\mathbf{X} \ \mathbf{X}']} \rangle. \quad (11)$$

Such coherent superposition of quantum states can be created using the quantum circuit shown in Fig. 5. This

circuit creates a superposition of $|\psi_0\rangle$ and $|\psi_1\rangle$ [27]:

$$|\Psi\rangle = \alpha \frac{\langle\chi|\psi_1\rangle}{|\langle\chi|\psi_1\rangle|} |\psi_0\rangle + \beta \frac{\langle\chi|\psi_0\rangle}{|\langle\chi|\psi_0\rangle|} |\psi_1\rangle. \quad (12)$$

Here, α and β are user-specified complex amplitudes, and $|\chi\rangle$ is a reference quantum state. This addition process is probabilistic. The success probability is $c_0c_1/(c_0 + c_1)$ if $\langle\psi_0|\psi_1\rangle = 0$, where $c_i = |\langle\chi|\psi_i\rangle|^2$. By recursively creating coherent superpositions of two states, we can construct the multi-state superposition $|\tilde{w}_r\rangle$ with $O(\text{poly } R)$ times of the quantum SVD (see Supplemental Material).

IV. CONCLUSION

The qDMD algorithm performs DMD on quantum time series data generated by a QLDES. This algorithm is also capable of computing (possibly complex) eigenvalues and eigenvectors of matrices. Excluding reference state preparation costs, the total gate complexity scales as $O(T \text{poly log}(NM/\epsilon) \text{poly}(R)/\epsilon^4)$. The qDMD algorithm can achieve an exponential speedup over its classical counterpart in terms of N if R remains at most $O(\text{poly log } N)$. Since the algorithm utilizes density matrix exponentiation and sampling-based inner product estimation, the dependency on ϵ is less optimal than that of the classical counterpart. Reducing the complexity with respect to ϵ should be addressed in future work.

ACKNOWLEDGMENTS

This work was supported by JST, PRESTO Grant Number JPMJPR2018, Japan, and partially by Crossover Alliance to Create the Future with People, Intelligence and Materials, Japan (to YM).

- [1] A. Y. Kitaev, Quantum measurements and the abelian stabilizer problem (1995), arXiv:quant-ph/9511026 [quant-ph].
- [2] R. Cleve, A. Ekert, C. Macchiavello, and M. Mosca, Quantum algorithms revisited, *Proceedings of the Royal Society of London. Series A: Mathematical, Physical and Engineering Sciences* **454**, 339 (1998).
- [3] D. S. Abrams and S. Lloyd, Quantum algorithm providing exponential speed increase for finding eigenvalues and eigenvectors, *Physical Review Letters* **83**, 5162 (1999).
- [4] S. Lloyd, M. Mohseni, and P. Rebentrost, Quantum principal component analysis, *Nature Physics* **10**, 631 (2014).
- [5] P. Rebentrost, A. Steffens, I. Marvian, and S. Lloyd, Quantum singular-value decomposition of nonsparse low-rank matrices, *Physical Review A* **97**, 012327 (2018).
- [6] A. W. Harrow, A. Hassidim, and S. Lloyd, Quantum algorithm for linear systems of equations, *Physical Review Letters* **103**, 150502 (2009).
- [7] A. M. Childs, R. Kothari, and R. D. Somma, Quantum algorithm for systems of linear equations with exponentially improved dependence on precision, *SIAM Journal on Computing* **46**, 1920 (2017).
- [8] A. Aspuru-Guzik, A. D. Dutoi, P. J. Love, and M. Head-Gordon, Simulated quantum computation of molecular energies, *Science* **309**, 1704 (2005).
- [9] M. Schuld, I. Sinayskiy, and F. Petruccione, Prediction by linear regression on a quantum computer, *Physical Review A* **94**, 022342 (2016).
- [10] D. W. Berry, High-order quantum algorithm for solving linear differential equations, *Journal of Physics A: Mathematical and Theoretical* **47**, 105301 (2014).
- [11] D. W. Berry, A. M. Childs, A. Ostrander, and G. Wang, Quantum algorithm for linear differential equations with exponentially improved dependence on precision, *Communications in Mathematical Physics* **356**, 1057 (2017).
- [12] A. M. Childs and J.-P. Liu, Quantum spectral methods for differential equations, *Communications in Mathematical Physics* **375**, 1291 (2020).

ical Physics **375**, 1427 (2020).

[13] J.-P. Liu, H. Ø. Kolden, H. K. Krovi, N. F. Loureiro, K. Trivisa, and A. M. Childs, Efficient quantum algorithm for dissipative nonlinear differential equations, Proceedings of the National Academy of Sciences **118**, e2026805118 (2021).

[14] S. L. Brunton, M. Budinić, E. Kaiser, and J. N. Kutz, Modern koopman theory for dynamical systems, SIAM Review **64**, 229 (2022).

[15] Y. T. Lin, R. B. Lowrie, D. Aslangil, Y. Subaşı, and A. T. Sornborger, Koopman von neumann mechanics and the koopman representation: A perspective on solving nonlinear dynamical systems with quantum computers (2022), arXiv:2202.02188 [quant-ph].

[16] A. Steffens, P. Rebentrost, I. Marvian, J. Eisert, and S. Lloyd, An efficient quantum algorithm for spectral estimation, New Journal of Physics **19**, 033005 (2017).

[17] C. Xue, Z.-Y. Chen, T.-P. Sun, X.-F. Xu, S.-M. Chen, H.-Y. Liu, X.-N. Zhuang, Y.-C. Wu, and G.-P. Guo, Quantum dynamic mode decomposition algorithm for high-dimensional time series analysis, Intelligent Computing **2**, 0045 (2023).

[18] H. Wang, L.-A. Wu, Y.-x. Liu, and F. Nori, Measurement-based quantum phase estimation algorithm for finding eigenvalues of non-unitary matrices, Physical Review A **82**, 062303 (2010).

[19] A. Daskin, A. Grama, and S. Kais, A universal quantum circuit scheme for finding complex eigenvalues, Quantum Information Processing **13**, 333 (2014).

[20] A. Teplukhin, B. K. Kendrick, and D. Babikov, Solving complex eigenvalue problems on a quantum annealer with applications to quantum scattering resonances, Physical Chemistry Chemical Physics **22**, 26136 (2020).

[21] C. Shao, Computing eigenvalues of diagonalizable matrices on a quantum computer, ACM Transactions on Quantum Computing **3**, 1 (2022).

[22] J. H. Tu, C. W. Rowley, D. Luchtenburg, S. L. Brunton, and J. N. Kutz, On dynamic mode decomposition: Theory and applications, Journal of Computational Dynamics **1**, 391 (2014).

[23] L. N. Trefethen and D. Bau, *Numerical linear algebra* (Society for Industrial and Applied Mathematics, Philadelphia, United States, 1997).

[24] M. A. Nielsen and I. L. Chuang, *Quantum Computation and Quantum Information* (Cambridge University Press, Cambridge, United Kingdom, 2010).

[25] D. Jennings, M. Lostaglio, R. B. Lowrie, S. Pallicher, and A. T. Sornborger, The cost of solving linear differential equations on a quantum computer: fast-forwarding to explicit resource counts (2023), arXiv:2309.07881 [quant-ph].

[26] S. Kimmel, C. Y.-Y. Lin, G. H. Low, M. Ozols, and T. J. Yoder, Hamiltonian simulation with optimal sample complexity, npj Quantum Information **3**, 13 (2017).

[27] M. Oszmaniec, A. Grudka, M. Horodecki, and A. Wójcik, Creating a superposition of unknown quantum states, Physical Review Letters **116**, 110403 (2016).